8348–8356 *Nucleic Acids Research, 2010, Vol. 38, No. 22* *Published online 18 August 2010*
doi:10.1093/nar/gkq731

Anti-tumor activity of splice-switching oligonucleotides

John A. Bauman[1,*], Shyh-Dar Li[2], Angela Yang[2], Leaf Huang[2] and Ryszard Kole[1,3]

[1]Department of Pharmacology and Lineberger Comprehensive Cancer Center, [2]Division of Molecular Pharmaceutics, School of Pharmacy, University of North Carolina, Chapel Hill, NC 27599 and [3]AVI BioPharma, Inc., Bothell, WA 98021, USA

Received May 11, 2010; Revised August 2, 2010; Accepted August 3, 2010

ABSTRACT

Alternative splicing has emerged as an important target for molecular therapies. Splice-switching oligonucleotides (SSOs) modulate alternative splicing by hybridizing to pre-mRNA sequences involved in splicing and blocking access to the transcript by splicing factors. Recently, the efficacy of SSOs has been established in various animal disease models; however, the application of SSOs against cancer targets has been hindered by poor *in vivo* delivery of antisense therapeutics to tumor cells. The apoptotic regulator Bcl-x is alternatively spliced to express anti-apoptotic Bcl-x_L and pro-apoptotic Bcl-x_S. Bcl-x_L is upregulated in many cancers and is associated with chemoresistance, distinguishing it as an important target for cancer therapy. We previously showed that redirection of Bcl-x pre-mRNA splicing from Bcl-x_L to -x_S induced apoptosis in breast and prostate cancer cells. In this study, the effect of SSO-induced Bcl-x splice-switching on metastatic melanoma was assessed in cell culture and B16F10 tumor xenografts. SSOs were delivered *in vivo* using lipid nanoparticles. Administration of nanoparticle with Bcl-x SSO resulted in modification of Bcl-x pre-mRNA splicing in lung metastases and reduced tumor load, while nanoparticle alone or formulated with a control SSO had no effect. Our findings demonstrate *in vivo* anti-tumor activity of SSOs that modulate Bcl-x pre-mRNA splicing.

INTRODUCTION

Over 90% of multi-exon pre-mRNA transcripts undergo alternative splicing (1) and up to one-half of disease-causing mutations affect splicing (2). Thus, in addition to its significant contribution to proteome diversity, alternative splicing constitutes an important therapeutic target (3). Splice-switching oligonucleotides (SSOs) modulate alternative splicing by hybridizing to pre-mRNA sequences involved in splicing and blocking access by various splicing factors (4,5). Unlike siRNA and traditional antisense approaches, which lead to RNA degradation by RISC and RNase H-mediated cleavage, respectively, direction of pre-mRNA splicing requires that the SSO-targeted RNA is not degraded. This is achieved by altering the oligonucleotide sugar-phosphate backbone as in, for example, the 2′-*O*-methoxyethyl (MOE) ribose modification (6,7). In order to realize their full therapeutic utility, SSOs must be efficiently delivered to the pharmacological site of action *in vivo* (8). This can be achieved by exploiting the inherent pharmacodynamic properties of the SSO chemistry (9,10), conjugation of cell penetrating peptides (11–13), and the use of nanoparticle carriers (14). As a result, *in vivo* efficacy has been established for SSOs in animal models of inflammatory disease, β-thalassemia and Duchenne muscular dystrophy (DMD) [For a recent review, see (15)], and early phase clinical trials using SSOs to treat DMD have yielded promising results (16,17).

Previously, this laboratory and others applied SSOs to manipulate the splicing pattern of the apoptotic regulator Bcl-x. Through alternative splicing, the Bcl-x gene yields two major protein isoforms with opposing functions, anti-apoptotic Bcl-x_L and pro-apoptotic Bcl-x_S (18) (Figure 1A). Bcl-x_L is upregulated in a number of cancers and confers resistance to a broad range of chemotherapeutic drugs (19). Bcl-x_S antagonizes the anti-apoptotic activity of Bcl-x_L and another anti-apoptotic protein, Bcl-2 (20,21). Redirection of Bcl-x splicing from Bcl-x_L to -x_S induced apoptosis and increased chemosensitivity in cancer cells in culture (22–24); however, the anti-tumor effect of this strategy remains to be demonstrated *in vivo*.

*To whom correspondence should be addressed. Tel: +1 919 966 4343; Fax: +1 919 966 5640; Email: john_bauman@med.unc.edu

The authors wish it to be known that, in their opinion, the first two authors should be regarded as joint First Authors.

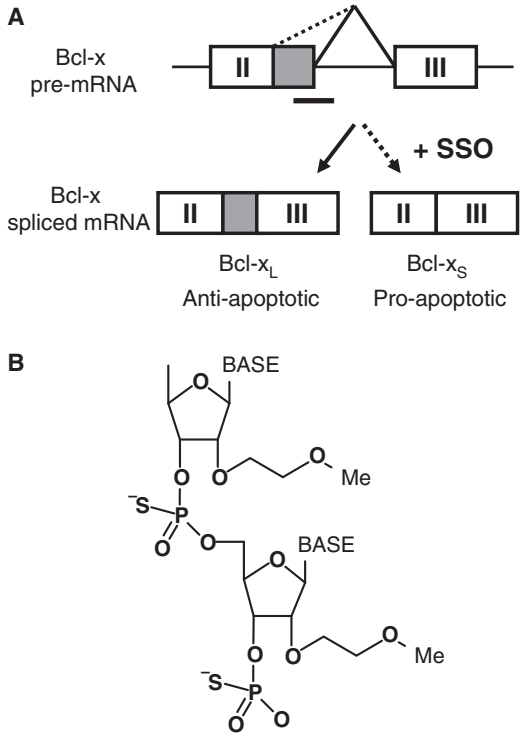

Figure 1. Direction of Bcl-x alternative splicing by SSO. (**A**) Use of the downstream or upstream alternative 5′-splice site within exon II of Bcl-x pre-mRNA yields anti-apoptotic Bcl-x_L or pro-apoptotic Bcl-x_S, respectively. SSO targeted to the downstream splice site redirects the splicing machinery to the upstream alternative splice site, resulting in a simultaneous decrease in production of Bcl-x_L and increase in production of Bcl-x_S. (**B**) Chemical structure of MOE phosphorothioate (PS) oligonucleotide. The MOE ribose modification confers RNase-H non-competence and increased affinity for target mRNA, while the PS inter-nucleotide linkage improves serum stability and bioavailability.

Because the SSO effectively converts Bcl-x_L to Bcl-x_S, cancers expressing high levels of Bcl-x_L represent good candidates for treatment with Bcl-x SSO (23). Metastatic melanoma is an aggressive malignancy with poor prognosis and disease progression is associated with increased Bcl-x_L expression (25,26). Xenografts of murine B16F10 melanoma cells provide a good model of this aggressive cancer because they express Bcl-x_L and are syngeneic to C57BL/6 mice, obviating the need for immunocompromised animals and providing a more realistic environment for drug testing. In this model, B16F10 murine melanoma cells localize to the lungs shortly after injection into the tail vein, providing a concise and predictable experimental time-course. In addition, the cell line used here expressed luciferase, providing an easily quantified measure of the tumor load. We previously failed to detect activity of systemically-delivered free SSOs in tumor xenografts. Thus, for this work we employed a liposome–DNA-polycation (LPD) nanoparticle (NP) formulation designed by the Huang laboratory (27–29), which delivered siRNA to tumor cells in the B16F10 xenograft model (30,31). In previous work, Huang and colleagues demonstrated enhanced tumor cell-specific uptake of this NP formulation by surface-modification with anisamide, a ligand of the sigma receptor, which is upregulated in many cancers (32,33) and is expressed in B16F10 cells (27,30,31,34).

Our findings show that delivery of Bcl-x SSO by the LPD NP resulted in modification of Bcl-x mRNA splicing in lung metastases and reduction of tumor load. This marks the first demonstration of SSO-induced splicing modification in tumor cells *in vivo* and provides support for Bcl-x splice-switching as a potential anti-tumor strategy.

MATERIALS AND METHODS

Materials

2′-*O*-methoxyethyl (MOE)-phosphorothioate SSOs (Figure 1B) were synthesized by ISIS Pharmaceuticals (Carlsbad, CA, USA). The Bcl-x SSO was targeted to the 5′-splice site of exon II in Bcl-x pre-mRNA (5′-TGG TTCTTACCCAGCCGCCG-3′, ISIS 105751) (35). An oligonucleotide targeted to aberrantly spliced human β-globin intron (5′-GCTATTACCTTAACCCAG-3′, ISIS 18204) (10) was used as negative control. For nanoparticle preparation cholesterol, protamine sulfate, calf thymus DNA and cloning water were purchased from Sigma-Aldrich (St Louis, MO, USA). DOTAP stock solution (20 mg/ml) was purchased from Avanti Polar Lipids (Alabaster, AL, USA).

Cell culture and transfection

B16F10 mouse melanoma cells expressing sigma receptors were used as model cells in this study (36). B16F10 cells stably expressing the firefly luciferase gene were provided by Dr Pilar Blancafort (University of North Carolina, Department of Pharmacology, NC, USA) (31). The cells were maintained in high-glucose Dulbecco's modified Eagle's medium supplemented with 10% fetal bovine serum and a 5% penicillin/streptomycin solution (GIBCO, Grand Island, NY, USA) at 37°C and 5% CO_2. Cells were seeded in 24- or 6-well plates at 7.0×10^5 and 5.0×10^5 cells/well, respectively, ~24 h prior to transfection. Cells were transfected with LipofectAmine 2000 (Invitrogen) in Opti-MEM (Invitrogen) per the manufacturer's recommendation.

RNA Isolation and analysis

Total RNA from cells or tissue was isolated using TRI Reagent (Molecular Research Center, Cincinnati, OH, USA) according to the manufacturer's protocol using 800 µl for ~5 mg tissue samples. Next, 200 ng of total RNA was subjected to RT–PCR (5′-CATGGCAGCAG TGAAGCAAG-3′, Bcl-x forward primer; 5′-GCATTGT TCCCGTAGAGATCC-3′, Bcl-x reverse primer; 5′-GTG CAGCGCAACCACGAGAC-3′, Mcl-1 forward primer; 5′-GCAGCACATTTCTGATGCCG-3′, Mcl-1 reverse primer) with rTth polymerase (Applied Biosystems, Foster City, CA, USA). Cycles of PCR proceeded at 95°C for 3 min, followed by 22 cycles of 95°C for 30 s, 56°C for 30 s, and 72°C for 1 min. The PCR contained Cy5-conjugated dCTP (GE Healthcare) for visualization. The PCR products were separated on a

10% non-denaturing polyacrylamide gel (Invitrogen) and bands were visualized on a Typhoon 9400 Imager (GE Healthcare). Images were quantified using ImageQuant analysis software (Version 5.2, Molecular Dynamics). The percentage of Bcl-x_S in each lane was determined by dividing the intensity of the 162-bp band (Bcl-x_S) by the total intensities of the 351 (Bcl-x_L) and 162-bp (Bcl-x_S) bands. The identity of the 162-bp band was confirmed by sequencing by the UNC-CH Genome Analysis Facility.

Cell viability assay

Cell viability in response to SSO treatment was assessed, with slight modifications, by a previously described clonogenic assay (23). Briefly, 24 h after oligonucleotide transfection in six-well plates, 250 cells were re-plated in 10-cm plates. After 10 days under normal culture conditions surviving colonies were stained with 2% methylene blue (Sigma) in 50% ethanol for 10 min. Colonies larger than 50 cells were counted. As a positive control for the assay, cells were treated with 1 μM staurosporine (STS).

Western blot analysis

Cells (5.0×10^5 cells/well in a six-well plate) were washed twice with ice-cold PBS and lysed in RIPA buffer (radioimmune precipitation assay buffer; 50 mM Tris–HCl, 150 mM NaCl, 5 mM EDTA, 1% Triton X-100, 0.1% SDS and 1% sodium deoxycholate) and a cocktail of protease inhibitors (Sigma). Total protein was quantified with the Quick Start Bradford Protein Assay Kit (Bio-Rad Laboratories, Inc., Hercules, CA, USA). Total protein (20 μg) was separated by electrophoresis on a 4–12% pre-cast Bis–Tris gel (Invitrogen) and electrotransferred to a polyvinylidene difluoride (PVDF) membrane. Membranes were stained with Ponceau's stain to confirm equal loading and transfer. Membranes were blocked for 1 h in BLOTTO (5% w/v non-fat dry milk in TBS, 0.1% Tween) or StartingBlock Buffer (Pierce) and incubated overnight at 4°C with primary antibodies: polyclonal Bcl-x antibody (1:2000; BD Transduction Labs), polyclonal PARP antibody (1:2000; Cell Signaling 9452) and mouse anti-β-actin monoclonal antibody (1:10 000; Sigma). Membranes were then incubated for 1 h with horseradish peroxidase-conjugated anti-mouse (1:100 000; Sigma) or goat anti-rabbit (1:10 000; Abcam) secondary antibodies. Blots were developed with ECL Plus reagents (GE Healthcare) and exposed to film (GE Healthcare). Bcl-x_L, Bcl-x_S, β-actin, cleaved PARP and full-length PARP migrated at 30, 22, 42, 89 and 116 kDa, respectively. β-Actin was used to confirm equal protein loading.

Preparation of SSO-containing nanoparticles

LPD NPs were prepared as described earlier (30,31). Briefly, naked NP were obtained by quickly mixing 150 μl suspension A (16.6 mM liposomes (DOTAP/cholesterol molar ratio = 1:1, and 400 μg/ml protamine in 5% dextrose) with 150 μl solution B (320 μg/ml oligonucleotide and 320 μg/ml calf thymus DNA in 5% dextrose) followed by incubation at room temperature for 10 min. The naked NP suspension (300 μl) was further incubated with 75.6 μl micellar solution of DSPE-PEG_{2000}-anisamide (10 mg/ml) [synthesized in the Huang lab as reported earlier (34)] at 50°C for 10 min and then allowed to stand at room temperature for 10 min. The resulting formulation was used within 20 min for the following experiments. These methods resulted in encapsulation of >90% oligoncuelotide or siRNA in previous studies (28,37,38).

Animal studies

Female C57BL/six mice of ages 6–8 weeks (16–18 g) were purchased from Charles River Laboratories (Wilmington, MA, USA). All experiments performed on the animals were in accordance with and approved by the Institutional Animal Care and Use Committee at the University of North Carolina. The mouse model was established by i.v. injection of 2×10^5 luciferase-expressing B16F10 cells on Day 0. Animals were i.v. injected with vehicle only (PBS), NP only (2.4 mg/kg), control or Bcl-x SSO NP (2.4 mg/kg), or free control or Bcl-x SSO (2.4 or 10 mg/kg) on Days 3–6 after tumor inoculation. On Day 7, some animals were euthanized for analysis of RNA splicing. For animals treated with free SSO, only RNA was analyzed. For animals treated with NP, blood was collected for analysis of toxicity marker. On Day 17 the remaining animals were euthanized for the analysis of tumor load. Tumor load was determined by measuring luciferase activity within tumor-bearing lungs, as described earlier (30,31).

Toxicity assays

Twenty-four hours after the final injection, blood samples were collected and serum was isolated. Analyses of serum aspartate aminotransferase (AST) and alanine aminotransferase (ALT) were performed at the Animal Clinical Laboratory Core Facility (University of North Carolina) using a Vitro 250 Chemical Analyzer (Ortho-Clinical Diagnostics, Rochester, NY, USA). Serum interleuikin-12 was measured with the enzyme-linked immunosorbant assay (ELISA) according to the manufacturer's protocol (BD Biosciences, San Diego, CA, USA). As a negative control, ALT/AST serum levels from untreated tumor-free mice were also measured.

Statistical analysis

Luciferase data were analyzed by one-way analysis of variance (ANOVA) and Tukey's post-test using Prism statistical software (GraphPad, version 4.03).

RESULTS

Modification of Bcl-x pre-mRNA in melanoma cells

Transfection of B16F10 cells with MOE-PS Bcl-x SSO targeted to the downstream 5′-splice site of Bcl-x exon 2 (Figure 1) induced a dose-dependant shift in splicing of Bcl-x pre-mRNA from anti-apoptotic Bcl-x_L to pro-apoptotic Bcl-x_S, while a control SSO had no effect on splicing (Figure 2A and B). Consistent with these results, probing of total protein from treated cells

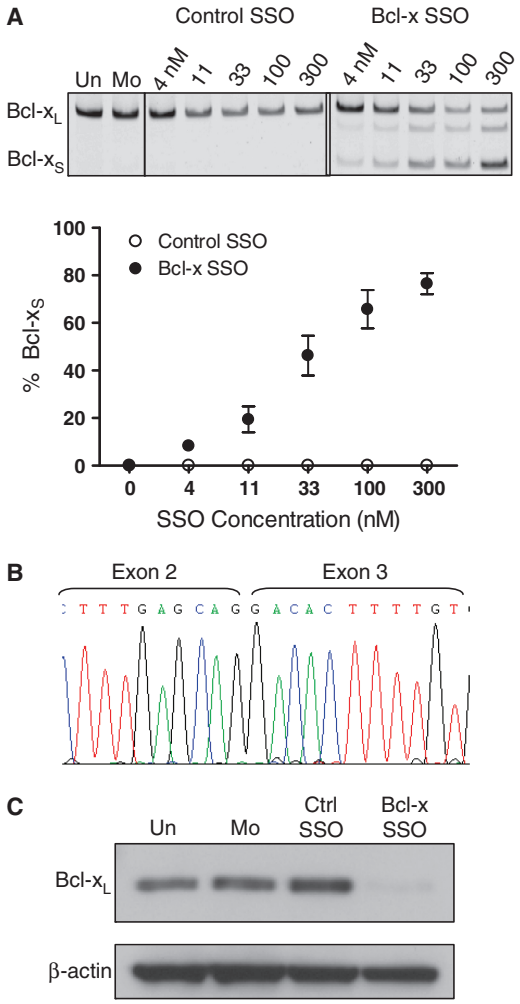

Figure 2. SSO induced Bcl-x splice-switching in B16F10 murine melanoma cells. (**A**) RT–PCR analysis of Bcl-x mRNA from cells transfected with control and Bcl-x SSO 24 h posttransfection. The Bcl-x SSO induces dose-dependant switching of Bcl-x mRNA splicing from anti-apoptotic Bcl-x_L to pro-apoptotic Bcl-x_S. Error bars indicate mean ± SD ($n = 3$). (**B**) Sequence analysis of the RT–PCR product corresponding to Bcl-x_S showing exons 2 and 3 joined at the upstream alternative splice site. (**C**) Immunoblot analysis of cells treated with 100 nM Bcl-x SSO 48 h posttransfection. The SSO induces a reduction in the Bcl-x_L protein isoform. Detection of β-actin confirms equal loading.

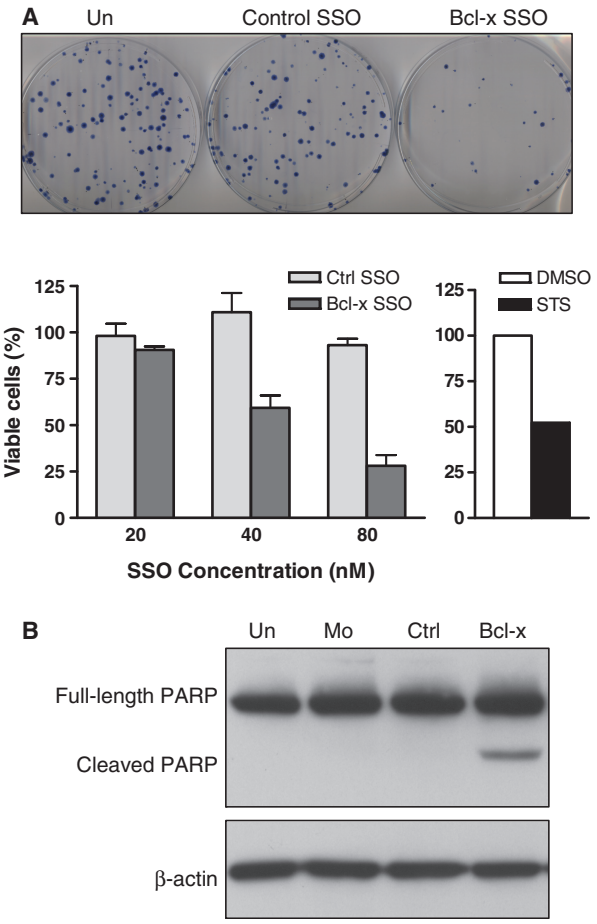

Figure 3. Bcl-x SSO induces cell death in B16F10 murine melanoma cells. (**A**) Effect of Bcl-x and control SSO on cell viability as determined by a clonogenic assay. Top panel shows images of representative plates at 80 nM concentration. Bottom left panel expresses viability of SSO-treated cells relative to untreated cells. Error bars indicate mean ± SD ($n = 3$–4). Bottom right panel shows viability of cells treated with 1 μM staurosporine (STS) relative to DMSO-treated cells. (**B**) Western blot of protein from cells treated with control and Bcl-x SSOs for 24 h. The presence of PARP cleavage in Bcl-x SSO-treated cells confirms that the observed decrease in cell viability is due to apoptosis. Detection of β-actin confirms equal loading.

with anti-Bcl-x antibody showed SSO-dependent reduction in the level Bcl-x_L protein (Figure 2C). We were unable to detect the expected Bcl-x_S protein because the endogenous level of murine Bcl-x_S expression was below the threshold required by available antibodies (Supplementary Figure S1). Importantly, SSO treatment resulted also in a dose-dependant decrease in cell viability, as evidenced by a clonogenic cell death assay (Figure 3A). This was accompanied by cleavage of poly (ADP-ribose) polymerase (PARP), indicating that the observed cell death was due to apoptosis (Figure 3B). These effects were absent in untreated and mock-transfected cells, and cells transfected with a control SSO. In addition, the Bcl-x SSO had no effect on the pre-mRNA splicing of Mcl-1, a closely related gene that shares sequence homology at the 5′-splice site, supporting sequence specificity of the Bcl-x SSO (Supplementary Figure S2).

Activity of Bcl-x SSO *in vivo*

To facilitate SSO delivery to cancer cells in tumor-bearing mice, an LPD NP developed by the Huang laboratory was used (30,31). The SSO and a carrier DNA (calf thymus DNA) were complexed by protamine into a compact core which was then coated with cationic lipids to form the NP (Figure 4). The surface of the NP was further modified with an anisamide ligand-conjugated polyethylene glycol (PEG)-lipid for targeting the sigma receptor-expressing B16F10 cells. This NP formulation could efficiently, specifically and with low toxicity deliver siRNA to tumor cells in the B16F10 tumor model, as shown earlier (30,31).

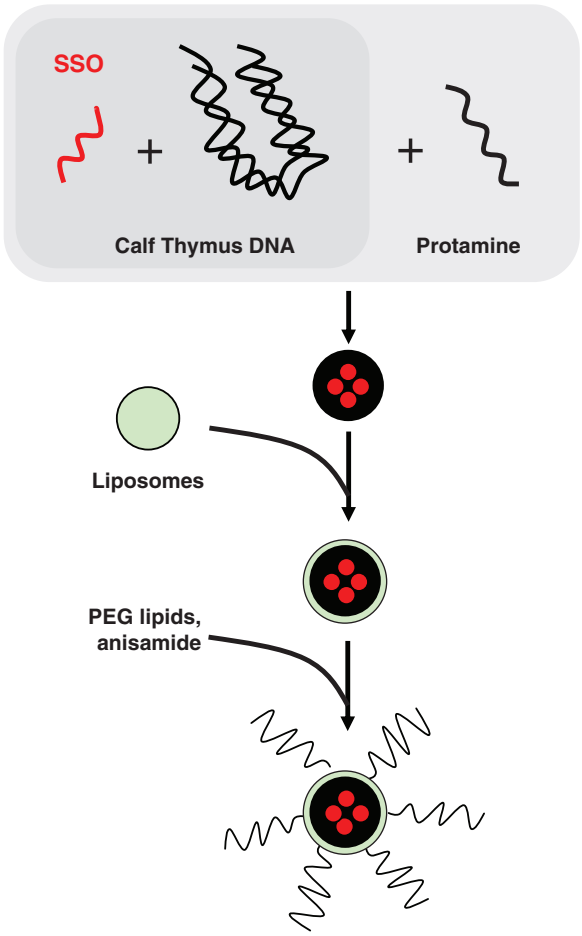

Figure 4. Schematic depiction of the preparation of SSO encapsulated LPD NP. The SSO was encapsulated into a condensed core with a high molecular weight polyanion (calf thymus DNA) and protamine, which was then coated with cationic liposomes. PEG lipids were inserted into the resultant bilayer to shield the positive charge and prevent aggregation in circulation. Anisamide, a commonly used targeting ligand that binds the sigma receptor, was conjugated to the distal end of the PEG lipids.

B16F10 murine melanoma cells localize in the lungs shortly after injection into the tail vein of C57BL/6 mice. In the absence of treatment, the mice die ~22 days following inoculation (30). This rapid course of disease dictated the treatment protocol ('Materials and Methods' section). RT–PCR analysis of total RNA from the tumor-bearing lungs of animals euthanized on Day 7 showed induction of Bcl-x_S mRNA expression in animals treated with the Bcl-x SSO NP formulation. This effect was dose-dependant, as increasing the number of injections resulted in a greater degree of Bcl-x splice-switching from Bcl-x_L to Bcl-x_S mRNA in the tumor nodules (Supplementary Figure S3). In contrast, Bcl-x_S mRNA levels in animals treated with control SSO NP formulation or free SSO were no different than in animals treated with PBS only (Figure 5A and Supplementary Figure S4). Modification of Bcl-x splicing in the liver was barely detectable in Bcl-x SSO NP-treated animals and undetectable in animals treated with control SSO NP or PBS only (Figure 5A). As a measure of tumor load, luciferase activity was assayed in lysates from tumor-bearing lungs of animals euthanized on Day 17. A dramatic reduction in luciferase activity was seen in animals treated with Bcl-x SSO NP compared to animals treated with NP only, control SSO NP, or PBS only (Figure 5B and C). Statistical analysis (ANOVA, Tukey's post-test) revealed that the reduction in luciferase activity in animals treated with Bcl-x SSO NP was significant compared to animals treated with PBS only ($P < 0.001$), NP only ($P < 0.05$) and control SSO NP ($P < 0.05$) (Figure 5B).

Toxicity studies

To determine the potential toxicities of NP and SSO treatment, serum levels of toxicity markers were analyzed in mice euthanized on Day 7 following tumor inoculation. Tissues with a leaky endothelial wall, such as the liver, allow significant uptake of NP (39). Accordingly, we analyzed serum aspartate aminotransferase (AST) and alanine aminotransferase (ALT) levels as markers of liver toxicity. Mean ALT and AST levels among treatment groups were within the normal range (Figure 6A and B). To test the possibility that components of the NP formulation might trigger an inflammatory response, serum levels of the pro-inflammatory cytokine IL-12 were also analyzed. Elevated IL-12 levels relative to the PBS control were observed in NP treatment groups (Empty NP, $P < 0.01$; Control SSO $P < 0.001$) (Figure 6C).

DISCUSSION

Alternative splicing has emerged as an important target for molecular therapies (15). Clinical trials using SSOs to treat DMD have yielded promising preliminary results (16,17), while numerous recent reports have confirmed the *in vivo* efficacy of SSOs in treating animal models of disease (15). SSOs have been applied against cancer targets *in vitro* (22,23,40), however *in vivo* validation of their efficacy has been hindered by the poor delivery of antisense therapeutics to tumor cells *in vivo* (8,41). Here we show that an SSO in LPD NP formulation was effective in delivery to tumor cells in the B16F10 model system (27,30,31).

Our data indicate that SSO-induced redirection of Bcl-x pre-mRNA splicing from Bcl-x_L to -x_S induced apoptosis and subsequent cell death in a dose-dependant manner in B16F10 melanoma cells in culture (Figures 2 and 3). *In vivo*, redirection of Bcl-x pre-mRNA splicing was associated with a significant reduction of tumor burden in rapidly growing and highly tumorigenic B16F10 lung metastases (Figure 5A–C). This finding is consistent with our *in vitro* data, as well as previous work in prostate and breast cancer cells (22,23). Interestingly, in this model both in cell culture and *in vivo* xenografts, modification of Bcl-x pre-mRNA splicing alone induced cell death, whereas in non-small cell lung carcinoma (A549) cells adjuvant chemotherapy was needed (24). Bcl-x_L expression may therefore be critical for survival of B16F10 cells, consistent with reports that increased Bcl-x_L expression is associated with melanoma progression and

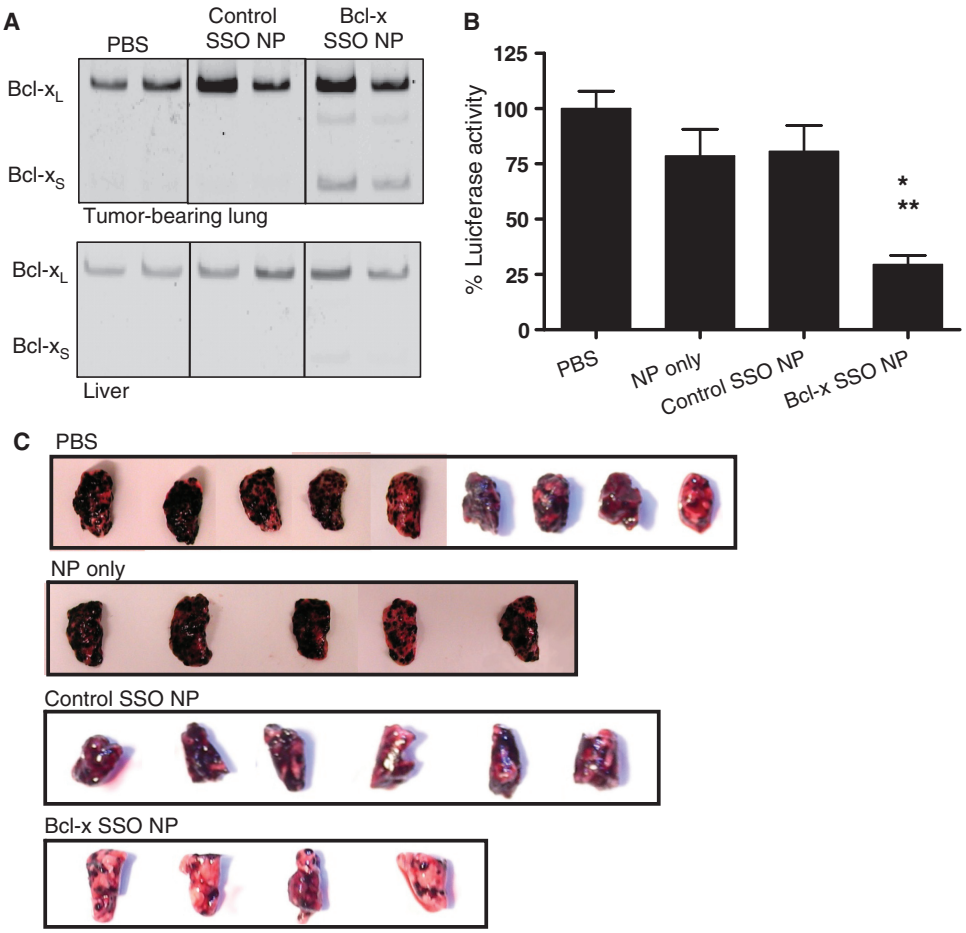

Figure 5. Effects of LPD-NP-delivered SSO in B16F10 tumor-bearing lungs. (**A**) RT–PCR analysis of Bcl-x mRNA splicing in the tumor-bearing lungs (upper panel) and liver (lower panel) of mice treated with vehicle only (PBS), empty NP, control SSO-formulated NP and Bcl-x SSO-formulated NP. (**B**) Luciferase activity in the tumor-loaded lungs on Day 17 after injections on Days 3–6. Asterisks denote statistical significance thresholds ($*P < 0.05$, $**P < 0.001$, determined by ANOVA and Tukey's posttest). Untreated $n = 26$, NP only $n = 8$, Control SSO NP $n = 13$, Bcl-x SSO NP $n = 9$. (**C**) Representative images of lungs excised from tumor-bearing mice on Day 17 following four injections of 2.4 mg/kg NP formulations on Days 3–6.

metastasis (25,26). Thus, other pharmacological agents that target Bcl-x_L may warrant further investigation in metastatic melanoma.

Our cell culture data are consistent with the predicted SSO mechanism of action. Namely, that Bcl-x SSO-induced modulation of Bcl-x pre-mRNA splicing reduced the level of Bcl-x_L, and increased the level of Bcl-x_S splice variants, causing apoptosis of cancer cells. This is evident at the RNA level, and is further supported by the dramatic reduction of Bcl-x_L protein and by induction of PARP cleavage (Figure 2C, 3C). Although SSO induced Bcl-x_S mRNA, we were unable to confirm concomitant production of Bcl-x_S protein by immunoblotting procedures. This was in spite of screening several commercially available antibodies and including attempts to concentrate the protein by immunoprecipitation prior to western analysis. This is likely because the maximum level of endogenous Bcl-x_S protein that could be induced by the SSO was below that which could be detected by available antibodies (Supplementary Figure S1).

In vivo, RT–PCR analysis of total RNA from tumor-bearing lungs demonstrated that Bcl-x splicing was shifted ~10% from Bcl-x_L to the -x_S splice variant. Yet this treatment led to marked reduction of tumor load in treated animals. Two interpretations of these results are possible. One, that *in vivo* even a minor reduction of Bcl-x_L levels and concomitant increase in Bcl-x_S, leads to death of cancer cells or at least inhibits their proliferation. However, it is also possible that the cells which took up the SSO more efficiently were more effectively killed by apoptosis and thus eliminated from the tissue subjected to subsequent analysis. If this is the case, RT–PCR underestimates the actual level of SSO-induced splice-switching.

BH3 mimetics comprise a novel class of cancer drugs that competitively antagonize the Bcl-2 anti-apoptotic proteins (42). For example, the small molecule ABT-737 binds Bcl-2, Bcl-x_L and Bcl-w proteins with nanomolar affinity. It induced apoptosis in lymphoma and small-cell lung carcinoma cells in culture, and caused tumor regression and improved survival in preclinical studies (43). By modifying the splicing pattern of Bcl-x, the SSO can

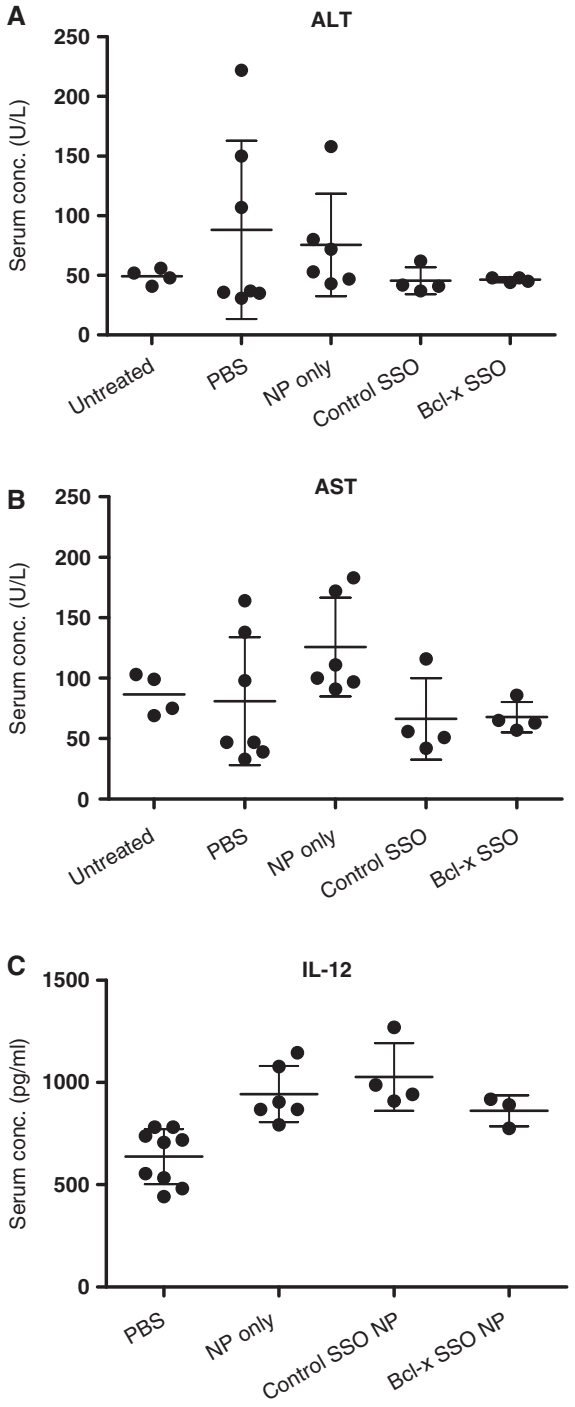

Figure 6. Serum enzyme and cytokine analysis. ALT (**A**), AST (**B**) and IL-12 (**C**) serum levels of untreated tumor-free and tumor-bearing C57BL/6 mice 24 h after the last of four consecutive daily treatments. Treatments consisted of i.v. injections of vehicle only (PBS), NP formulated with control SSO, or NP formulated with SSO targeted to Bcl-x.

be thought of as prompting the tumor cell to produce an endogenous BH3 mimetic, Bcl-x_S, capable of antagonizing Bcl-2 and Bcl-x_L and promoting apoptosis.

NPs are known to accumulate non-specifically in the liver due to the fenestrated vasculature (39). We did not observe significant Bcl-x splice-switching in the liver (Figure 5A), and ALT and AST serum levels of the treatment groups was within the normal range (Figure 6A and B). This suggests that liver uptake of the NP was limited and did not translate into significant biological activity or toxicity. In some tumor-bearing, control mice AST and AST values were >100 U/L suggesting that this could be a rare response to tumor burden. We did detect a modest elevation of serum IL-12 levels in NP treatment groups relative to the PBS control (Figure 6C). A previous report with the LPD NP showed more pronounced induction of inflammatory toxicity at doses ≥ 1.2 mg/kg (29,30). However, that study analyzed local toxicity from lung lysate, whereas we analyzed serum from systemic circulation. It is unclear whether this small but statistically significant increase is biologically relevant. Elevated IL-12 could be due to unmethylated CpG motifs present in the calf thymus DNA component of the NP. While we cannot exclude the possibility that the observed IL-12 increase contributed to the antitumor effect of the Bcl-x SSO, this seems unlikely because IL-12 induction was observed in all NP treatment groups, whereas reduction of tumor load was only evident in animals treated with the Bcl-x SSO.

The inclusion of calf thymus DNA in the NP complicates the use of this formulation from a pharmaceutics and regulatory perspective. Recently, Chono *et al.* (38) replaced calf thymus DNA with a high molecular weight anionic polysaccharide, hyaluronic acid, resulting in a NP containing cationic liposome, protamine and hyaluronic acid (LPH). The LPH formulation delivered siRNA *in vivo* with potency similar to that of the LPD formulation; however, induction of both IL-6 and IL-12 cytokines by LPH was significantly lower than that of the corresponding LPD containing the calf thymus DNA. The LPH NP formulation could be employed for delivery of SSOs and other antisense therapeutics to tumors in future studies.

Our results extend previous findings on the LPD NP formulation, which delivered siRNA to the cytoplasm, the site of dicer activity, to oligonucleotides that function in the nucleus, the site of splicing modulation. Thus, through delivery of SSOs, liposome-based NP formulations may be used not only to downregulate, but also to upregulate endogenous gene expression, as is evidenced by the induction of Bcl-x_S mRNA we observed. In addition, our findings are consistent with Bcl-x pre-mRNA splice switching as a possible anti-tumor strategy in melanoma as well as other malignancies expressing Bcl-x_L.

SUPPLEMENTARY DATA

Supplementary Data are available at NAR Online.

ACKNOWLEDGEMENTS

The authors thank Dr Rudy Juliano from UNC for critical reading of the manuscript. The authors thank Dr Brett Monia for a kind gift of 2′-*O*-MOE

oligonucleotides used in this work and Jennifer Roberts for technical assistance.

FUNDING

American Heart Association (predoctoral fellowship to J.A.B.); National Institutes of Health (PO1-GM-59299 to R.K.; R01-CA129835 to L.H.). Funding for open access charge: National Institutes of Health (PO1-GM-59299).

Conflict of interest statement. R.K. is a full-time employee of AVI Biopharma Inc., Bothell, WA, USA, a company that develops RNA-based drugs.

REFERENCES

1. Wang,E.T., Sandberg,R., Luo,S., Khrebtukova,I., Zhang,L., Mayr,C., Kingsmore,S.F., Schroth,G.P. and Burge,C.B. (2008) Alternative isoform regulation in human tissue transcriptomes. *Nature*, **456**, 470–476.
2. Lopez-Bigas,N., Audit,B., Ouzounis,C., Parra,G. and Guigo,R. (2005) Are splicing mutations the most frequent cause of hereditary disease? *FEBS Lett*., **579**, 1900–1903.
3. Cooper,T.A., Wan,L. and Dreyfuss,G. (2009) RNA and disease. *Cell*, **136**, 777–793.
4. Dominski,Z. and Kole,R. (1993) Restoration of correct splicing in thalassemic pre-mRNA by antisense oligonucleotides. *Proc. Natl Acad. Sci. USA*, **90**, 8673–8677.
5. Sierakowska,H., Sambade,M.J., Agrawal,S. and Kole,R. (1996) Repair of thalassemic human beta-globin mRNA in mammalian cells by antisense oligonucleotides. *Proc. Natl Acad. Sci. USA*, **93**, 12840–12844.
6. Sazani,P., Astriab-Fischer,A. and Kole,R. (2003) Effects of base modifications on antisense properties of 2′-O-methoxyethyl and PNA oligonucleotides. *Antisense Nucleic Acid Drug. Dev*., **13**, 119–128.
7. Sazani,P., Kang,S.H., Maier,M.A., Wei,C., Dillman,J., Summerton,J., Manoharan,M. and Kole,R. (2001) Nuclear antisense effects of neutral, anionic and cationic oligonucleotide analogs. *Nucleic Acids Res*., **29**, 3965–3974.
8. Juliano,R.L., Bauman,J., Kang,H. and Ming,X. (2009) Biological barriers to therapy with antisense and siRNA oligonucleotides. *Mol. Pharm*., **6**, 686–695.
9. Graziewicz,M.A., Tarrant,T.K., Buckley,B., Roberts,J., Fulton,L., Hansen,H., Orum,H., Kole,R. and Sazani,P. (2008) An endogenous TNF-alpha antagonist induced by splice-switching oligonucleotides reduces inflammation in hepatitis and arthritis mouse models. *Mol. Ther*., **16**, 1316–1322.
10. Sazani,P., Gemignani,F., Kang,S.H., Maier,M.A., Manoharan,M., Persmark,M., Bortner,D. and Kole,R. (2002) Systemically delivered antisense oligomers upregulate gene expression in mouse tissues. *Nat. Biotechnol*., **20**, 1228–1233.
11. Jearawiriyapaisarn,N., Moulton,H.M., Buckley,B., Roberts,J., Sazani,P., Fucharoen,S., Iversen,P.L. and Kole,R. (2008) Sustained dystrophin expression induced by peptide-conjugated morpholino oligomers in the muscles of mdx mice. *Mol. Ther*., **16**, 1624–1629.
12. Wu,B., Moulton,H.M., Iversen,P.L., Jiang,J., Li,J., Li,J., Spurney,C.F., Sali,A., Guerron,A.D., Nagaraju,K. *et al*. (2008) Effective rescue of dystrophin improves cardiac function in dystrophin-deficient mice by a modified morpholino oligomer. *Proc. Natl Acad. Sci. USA*, **105**, 14814–14819.
13. Svasti,S., Suwanmanee,T., Fucharoen,S., Moulton,H.M., Nelson,M.H., Maeda,N., Smithies,O. and Kole,R. (2009) RNA repair restores hemoglobin expression in IVS2-654 thalassemic mice. *Proc. Natl Acad. Sci. USA*, **106**, 1205–1210.
14. Rimessi,P., Sabatelli,P., Fabris,M., Braghetta,P., Bassi,E., Spitali,P., Vattemi,G., Tomelleri,G., Mari,L., Perrone,D. *et al*. (2009) Cationic PMMA nanoparticles bind and deliver antisense oligoribonucleotides allowing restoration of dystrophin expression in the mdx mouse. *Mol. Ther*., **17**, 820–827.
15. Bauman,J., Jearawiriyapaisarn,N. and Kole,R. (2009) Therapeutic potential of splice-switching oligonucleotides. *Oligonucleotides*, **19**, 1–14.
16. van Deutekom,J.C., Janson,A.A., Ginjaar,I.B., Frankhuizen,W.S., Aartsma-Rus,A., Bremmer-Bout,M., den Dunnen,J.T., Koop,K., van der Kooi,A.J., Goemans,N.M. *et al*. (2007) Local dystrophin restoration with antisense oligonucleotide PRO051. *N. Engl. J. Med*., **357**, 2677–2686.
17. Kinali,M., Arechavala-Gomeza,V., Feng,L., Cirak,S., Hunt,D., Adkin,C., Guglieri,M., Ashton,E., Abbs,S., Nihoyannopoulos,P. *et al*. (2009) Local restoration of dystrophin expression with the morpholino oligomer AVI-4658 in Duchenne muscular dystrophy: a single-blind, placebo-controlled, dose-escalation, proof-of-concept study. *Lancet Neurol*., **8**, 918–928.
18. Boise,L.H., Gonzalez-Garcia,M., Postema,C.E., Ding,L., Lindsten,T., Turka,L.A., Mao,X., Nunez,G. and Thompson,C.B. (1993) bcl-x, a bcl-2-related gene that functions as a dominant regulator of apoptotic cell death. *Cell*, **74**, 597–608.
19. Amundson,S.A., Myers,T.G., Scudiero,D., Kitada,S., Reed,J.C. and Fornace,A.J. Jr (2000) An informatics approach identifying markers of chemosensitivity in human cancer cell lines. *Cancer Res*., **60**, 6101–6110.
20. Lindenboim,L., Borner,C. and Stein,R. (2001) Bcl-x(S) can form homodimers and heterodimers and its apoptotic activity requires localization of Bcl-x(S) to the mitochondria and its BH3 and loop domains. *Cell Death Differ*., **8**, 933–942.
21. Minn,A.J., Boise,L.H. and Thompson,C.B. (1996) Bcl-x(S) anatagonizes the protective effects of Bcl-x(L). *J. Biol. Chem*., **271**, 6306–6312.
22. Mercatante,D.R., Bortner,C.D., Cidlowski,J.A. and Kole,R. (2001) Modification of alternative splicing of Bcl-x pre-mRNA in prostate and breast cancer cells. analysis of apoptosis and cell death. *J. Biol. Chem*., **276**, 16411–16417.
23. Mercatante,D.R., Mohler,J.L. and Kole,R. (2002) Cellular response to an antisense-mediated shift of Bcl-x pre-mRNA splicing and antineoplastic agents. *J. Biol. Chem*., **277**, 49374–49382.
24. Taylor,J.K., Zhang,Q.Q., Wyatt,J.R. and Dean,N.M. (1999) Induction of endogenous Bcl-xS through the control of Bcl-x pre-mRNA splicing by antisense oligonucleotides. *Nat. Biotechnol*., **17**, 1097–1100.
25. Zhuang,L., Lee,C.S., Scolyer,R.A., McCarthy,S.W., Zhang,X.D., Thompson,J.F. and Hersey,P. (2007) Mcl-1, Bcl-XL and Stat3 expression are associated with progression of melanoma whereas Bcl-2, AP-2 and MITF levels decrease during progression of melanoma. *Mod. Pathol*., **20**, 416–426.
26. Leiter,U., Schmid,R.M., Kaskel,P., Peter,R.U. and Krahn,G. (2000) Antiapoptotic bcl-2 and bcl-xL in advanced malignant melanoma. *Arch. Dermatol. Res*., **292**, 225–232.
27. Li,S.D. and Huang,L. (2006) Surface-modified LPD nanoparticles for tumor targeting. *Ann. NY Acad. Sci*., **1082**, 1–8.
28. Li,S.D. and Huang,L. (2006) Targeted delivery of antisense oligodeoxynucleotide and small interference RNA into lung cancer cells. *Mol. Pharm*., **3**, 579–588.
29. Li,S.D., Chen,Y.C., Hackett,M.J. and Huang,L. (2008) Tumor-targeted delivery of siRNA by self-assembled nanoparticles. *Mol. Ther*., **16**, 163–169.
30. Li,S.D., Chono,S. and Huang,L. (2008) Efficient oncogene silencing and metastasis inhibition via systemic delivery of siRNA. *Mol. Ther*., **16**, 942–946.
31. Li,S.D., Chono,S. and Huang,L. (2008) Efficient gene silencing in metastatic tumor by siRNA formulated in surface-modified nanoparticles. *J. Control Release*, **126**, 77–84.
32. John,C.S., Bowen,W.D., Varma,V.M., McAfee,J.G. and Moody,T.W. (1995) Sigma receptors are expressed in human non-small cell lung carcinoma. *Life Sci*., **56**, 2385–2392.
33. Vilner,B.J., John,C.S. and Bowen,W.D. (1995) Sigma-1 and sigma-2 receptors are expressed in a wide variety of human and rodent tumor cell lines. *Cancer Res*., **55**, 408–413.
34. Banerjee,R., Tyagi,P., Li,S. and Huang,L. (2004) Anisamide-targeted stealth liposomes: a potent carrier for

targeting doxorubicin to human prostate cancer cells. *Int. J. Cancer*, **112**, 693–700.
35. Zhang,N., Peairs,J.J., Yang,P., Tyrrell,J., Roberts,J., Kole,R. and Jaffe,G.J. (2007) The importance of Bcl-xL in the survival of human RPE cells. *Invest. Ophthalmol. Vis. Sci.*, **48**, 3846–3853.
36. Pham,T.Q., Berghofer,P., Liu,X., Greguric,I., Dikic,B., Ballantyne,P., Mattner,F., Nguyen,V., Loc'h,C. and Katsifis,A. (2007) Preparation and biologic evaluation of a novel radioiodinated benzylpiperazine, 123I-MEL037, for malignant melanoma. *J. Nucl. Med.*, **48**, 1348–1356.
37. Li,S.D. and Huang,L. (2009) Nanoparticles evading the reticuloendothelial system: role of the supported bilayer. *Biochim. Biophys. Acta*, **1788**, 2259–2266.
38. Chono,S., Li,S.D., Conwell,C.C. and Huang,L. (2008) An efficient and low immunostimulatory nanoparticle formulation for systemic siRNA delivery to the tumor. *J. Control Release*, **131**, 64–69.
39. Li,S.D. and Huang,L. (2008) Pharmacokinetics and biodistribution of nanoparticles. *Mol. Pharm.*, **5**, 496–504.
40. Wan,J., Sazani,P. and Kole,R. (2009) Modification of HER2 pre-mRNA alternative splicing and its effects on breast cancer cells. *Int. J. Cancer*, **124**, 772–777.
41. Bennett,C.F. (2008) In Crooke,S.T. (ed.), *Antisense Drug Technology: Principles, Strategies, and Applications*, 2nd edn. CRC Press, Boca Raton, FL, pp. 273–304.
42. Chonghaile,T.N. and Letai,A. (2008) Mimicking the BH3 domain to kill cancer cells. *Oncogene*, **27(Suppl 1)**, S149–S157.
43. Oltersdorf,T., Elmore,S.W., Shoemaker,A.R., Armstrong,R.C., Augeri,D.J., Belli,B.A., Bruncko,M., Deckwerth,T.L., Dinges,J., Hajduk,P.J. *et al.* (2005) An inhibitor of Bcl-2 family proteins induces regression of solid tumours. *Nature*, **435**, 677–681.